

A Precision Io Monitor System at the SRRC

C.K. Kuan^{*}, D.J. Wang^{*}, S.Y. Perng^{*}, J. Wang^{*}, C.J. Lin^{*}, J.R. Chen^{*,#}

^{*}Synchrotron Radiation Research Center (SRRC), No.1 R&D Road VI, Science-Based Industrial Park, Hsinchu 300, Taiwan.
Phone: (886) 3-5780281; Fax: (886) 3-5783890
E-mail: ckkuan@srcc.gov.tw

[#]Department of Nuclear Science, National Tsing-Hua University, Hsinchu 300, Taiwan.

Abstract

A photon beam intensity monitor (Io monitor) system always consists of a mirror, a pinhole, a photodiode, and a scanning mechanism. The mechanical fluctuation, thermal fluctuation or the resolution of scanning mechanism usually affects the reliability of the Io monitor system. A precision Io monitor system is needed to indicate the photon beam intensity fluctuation when the photon beam intensity fluctuation is down to 0.1% at the photon beam line. In the study on the precision Io monitor system used an independent manipulator to isolate the mechanical fluctuations from beam-line chamber. The thermal fluctuations were reduced by a precision cooling water system and a precision Air Handling Unit (AHU). A resolution 0.1 μ m piezo-actuated flexible stage enhanced the scanning mechanism. This precision Io monitor system was proved to be able to detect the photon beam intensity fluctuation < 0.1%.

Keywords: Io monitor, mechanical stability

1. Introduction

The Taiwan Light Source (TLS) at the SRRC aims for a photon beam intensity fluctuation of ~0.1% at the photon beam line. A precision Io monitor system is needed to index the photon stability. TLS has established the index of the short-term photon beam stability using an Automatic Peak Tracking System (APTS) of photon profile [1-2]. A dedicated diagnostic beam line is built next to Low-energy Spherical Grating Mirror beam line, LSGM. APTS is built for the demand that most of the synchrotron light users need the short-term peak-to-peak beam stability well within 0.5%. The mechanical and thermal fluctuations affecting the stability of the mechanical system are studied at the SRRC [3]. A precision Io monitor system should reduce the mechanical and thermal fluctuations and increase the resolution of the scanning mechanism.

In our design of precision Io monitor system, it consisted of a Vertical Focusing Mirror (VFM) supported by an independent manipulator [4], a pinhole, a photodiode, a precision scanning mechanism, and a precision cooling water system. The incident photons were focused by VFM and detected by a photodiode positioned behind a 50 μ m pinhole. The pinhole was located precisely at the focused point by the precision scanning mechanism. The precision scanning mechanism consisted of a resolution 2 μ m stepping motor stage and a resolution 0.1 μ m piezo-actuated flexible stage. The independent manipulator isolated the vibration and thermal deformation from the VFM chamber. The air temperature of the diagnostic beam line area was isolated using an independent AHU to keep the air temperature fluctuations to < \pm 0.1 $^{\circ}$ C. The VFM, pinhole, and photodiode were cooled by precision cooling water system with a temperature fluctuation of < \pm 0.01 $^{\circ}$ C.

2. Mechanical Stability

To increase the sensitivity of Io monitor system, the VFM is needed to focus the beam size. The mechanical stability of VFM is influenced by the surrounding vibration, air temperature, and cooling water temperature. If the VFM has vertical angle fluctuation, the position of focused beam spot at the pinhole will be changed. When this vertical angle fluctuation is bigger than the beam fluctuation, the Io monitor system will give the wrong information of beam stability to users. The readings of Io monitor system become the information of VFM mechanical stability, not the beam stability. To keep the mechanical stability of VFM is very important. In the VFM mechanism's design, the independent manipulator, with vacuum bellows, isolated the vibration and thermal deformation from the VFM chamber. The holder of VFM used the low thermal expansion material Invar to reduce the thermal effect. The VFM was cooled using side cooling method. The interfaces between VFM and side cooling plates were very compact contact using the Indium foils and precision fixture to obtain high thermal conduction and to prevent the crack of VFM. Figure 1 is the temperature distribution after the photon beam exposed on the VFM surface when beam current is 200mA, using the commercial program ANSYS. The maximum temperature is 127 °C in the center of VFM surface. Figure 2 is the VFM deformation according the thermal analysis in the Figure 1. The deformation is very small.

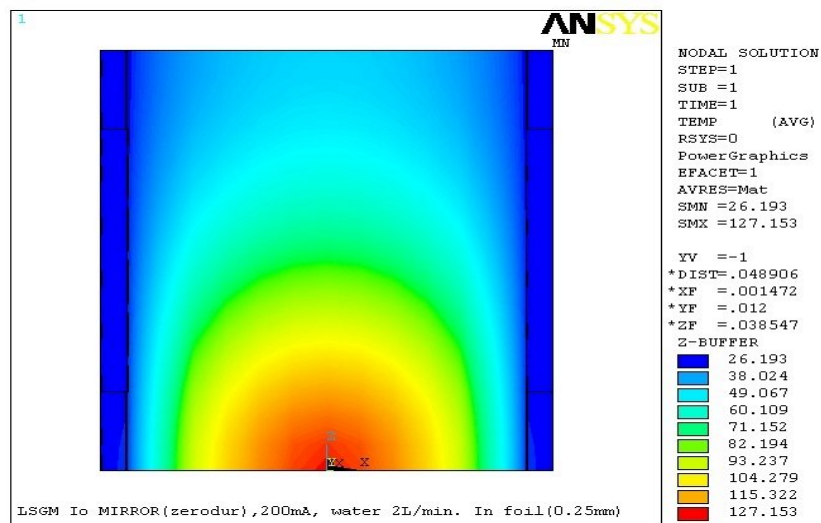


Fig.1: Temperature distribution after the photon beam exposed on the VFM surface when beam current is 200mA.

The thermal coefficient of steel is about 11 ppm/°C. This is very big for the thermal deformation problems. To minimize the thermal deformation of the steel pedestal supporting the Io monitor system, the pedestal's thermal time constant must be as big as possible. This thermal time constant can be increased by adding the pedestal's weight, filling the inside of the pedestal with water, and decreasing the thermal film coefficient with a static airflow layer on the pedestal's surface. The air temperature of the diagnostic beam line area was separated with the experiment area by plastics. An independent Air

Handling Unit (AHU) was installed to keep the air temperature fluctuations to $\leq \pm 0.1$ °C as shown in the Figure 3 (upper fig.).

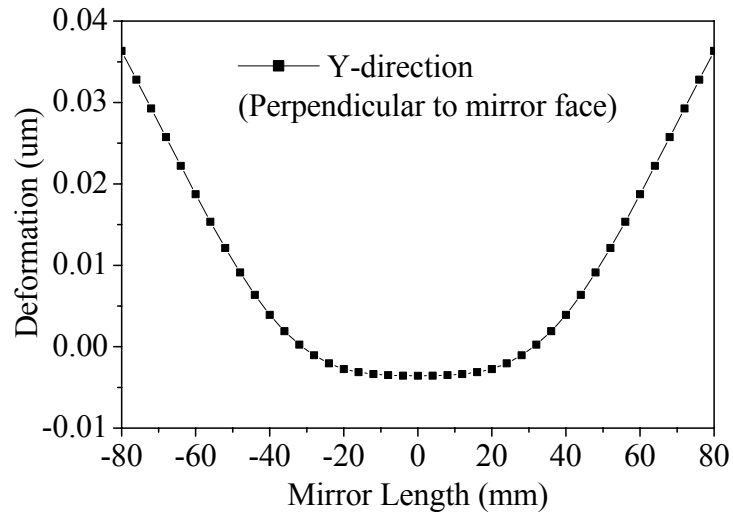


Fig. 2: VFM deformation after the photon beam exposed on the VFM surface.

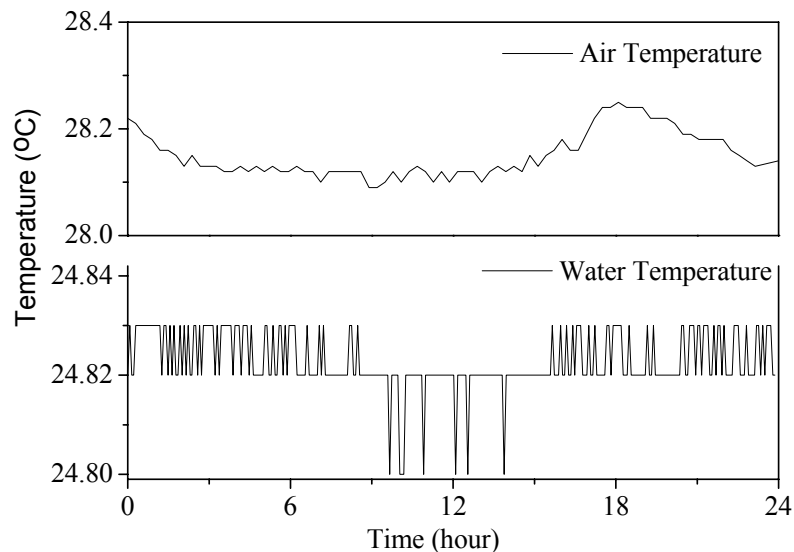


Fig. 3: The air temperature of the diagnostic beam line area (upper fig.). The cooling water temperature used in VFM, pinhole and photodiode (lower fig.).

The temperature fluctuations of cooling water induced the thermal deformation and the reliability of the precision Io monitor system. All the VFM, pinhole, and photodiode were cooled by a precision cooling water system with a temperature fluctuation of $< \pm 0.01$ °C as shown in Figure 3 (lower fig.).

The intensity of photon beam was decayed with time. This meant the thermal loads on the VFM, pinhole, and photodiode were dependant with time. Figure 4 was the positions of the focused beam spot in one user shift (8 hours) using the APTS, the

scanning motor was a resolution $2\mu\text{m}$ stepping motor. The position variations in this condition were always over $100\mu\text{m}$. Figure 5 was the positions of the focused beam spot in one user shift using the precision Io monitor system, but only the resolution $2\mu\text{m}$ stepping motor was executed during the scanning procedure. The position variations in this condition were below $\pm 4\mu\text{m}$. The mechanical stability was well improvement.

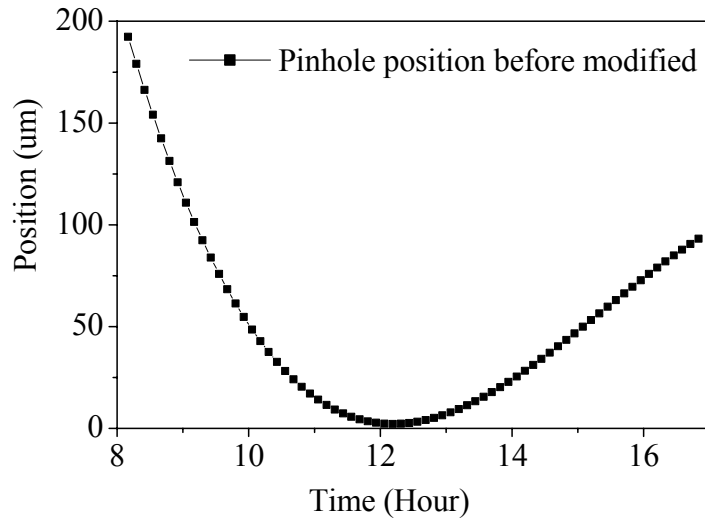


Fig. 4: The position of the focused beam spot in one user shift using the APTS, the scanning motor was resolution $2\mu\text{m}$ stepping motor.

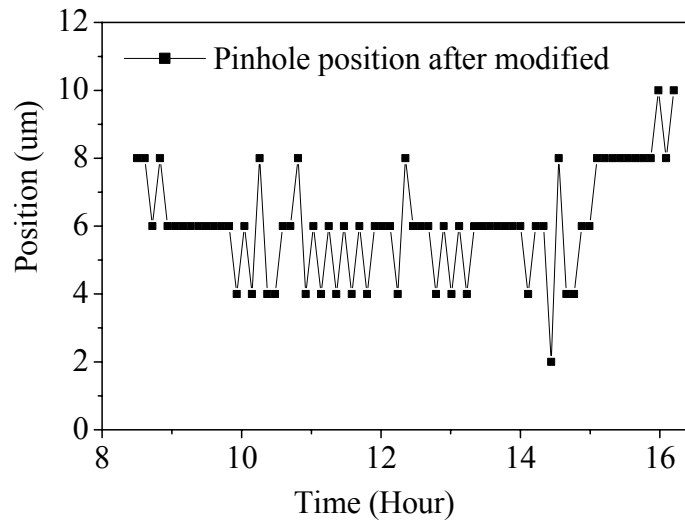


Fig. 5: The position of the focused beam spot in one user shift using the precision Io monitor system, but only the resolution $2\mu\text{m}$ stepping motor was executed.

3. The Reliability of Scanning Procedure

3.1 Definition of dI_o/I_o

The dI_o/I_o is an index of beam photon stability at TLS. The I_o is defined as the photon-current detected by the photodiode and the dI_o is the current deviation due to the electron beam instability. The I_o data are taken in 2 Hz sampling rates every 256 seconds. The definition of de-trended information is to eliminate the decay effect of beam current. The value of dI_o/I_o is calculated by de-trended information with full width root mean square (FWRMS) divided by the average value, which can be represented as:

$$dI_o / I_o = 2 * \frac{\sqrt{\sum_{i=1}^N (x_i - \bar{x})^2 / N}}{(\sum_{i=1}^N x_i) / N}$$

where N is the number of data points, x_i is the de-trended data sampled at 2 Hz.

3.2 The Performance of Scanning Mechanism

The precision scanning mechanism consisted of stepping motor stage and piezo-actuated flexible stage. The resolution of stepping motor stage was $2\mu\text{m}$ for the rough scan within the range $\pm 40\mu\text{m}$. Figure 6 was the performance of the stepping motor stage, the motor backlash was $2\mu\text{m}$ and the maximum root mean square (RMS) was $0.28\mu\text{m}$. The resolution of piezo-actuated flexible stage was $0.1\mu\text{m}$ for the precise scan within the range $\pm 5\mu\text{m}$. Figure 7 showed the performance of the piezo-actuated flexible stage, the maximum root mean square (RMS) was $0.15\mu\text{m}$.

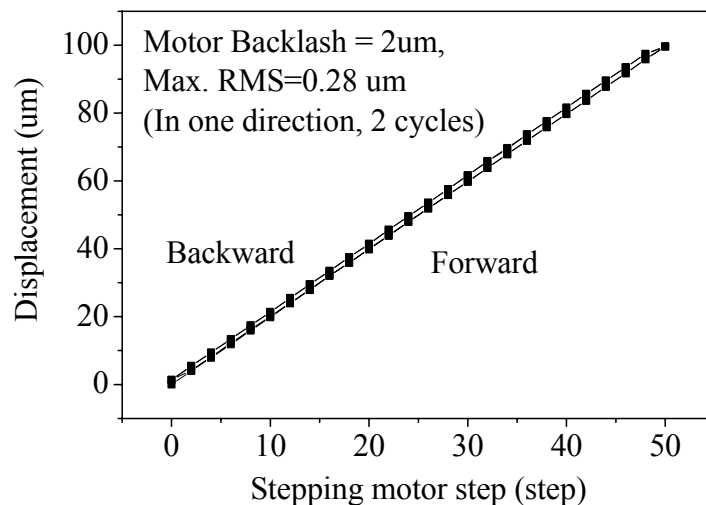


Fig. 6: The performance of the resolution $2\mu\text{m}$ stepping motor stage.

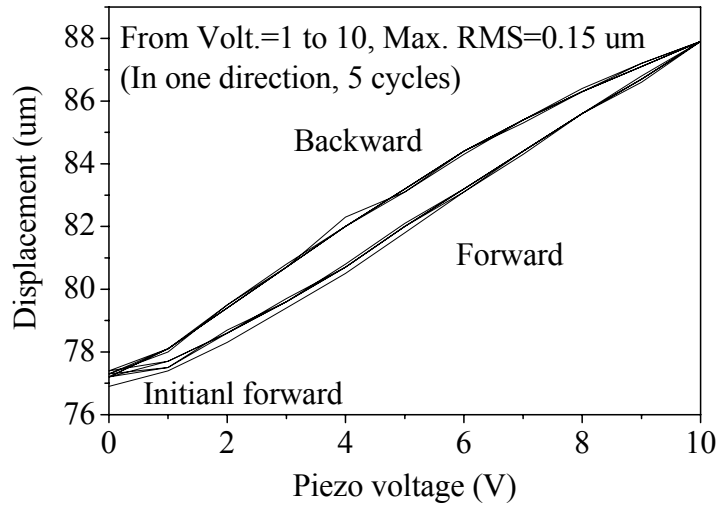


Fig. 7: The performance of the resolution $0.1\mu\text{m}$ piezo-actuated flexible stage.

3.3 The Offset Effect of Pinhole

The radiated photon beam from a bending magnet is wide spread in horizontal direction. The major concern of the photon intensity fluctuation is in the vertical direction distributed as Gaussian profile. After scanning procedure, the center point of the pinhole should be located in the top point of Gaussian profile and stays in this point for 256 seconds to take the I_0 data. If there is a pinhole offset between the two points, there will have an offset effect of pinhole. Figure 8 is the simulation of the offset effect of pinhole, the pinhole offsets are from 0 to $3.5\mu\text{m}$ and the beam variations are 1 and $2\mu\text{m}$. The photon intensity variation is proportional to the pinhole offset.

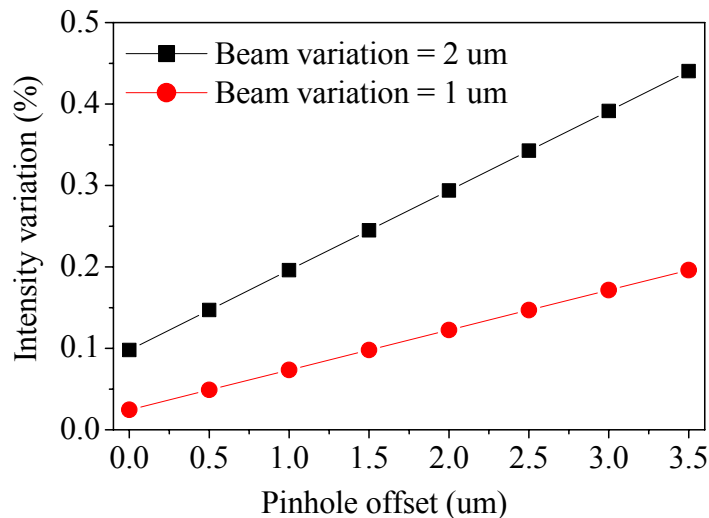


Fig. 8: The photon intensity variation proportional to the pinhole offset.

For observing the phenomena of offset effect easily, the I_0 data were subtracted from the low frequency (0.2Hz); the remaining data were induced by high frequency. With the resolution of 0.1 μ m piezo-actuated flexible stage, the experiments of offset effect were implemented. Figure 9 showed the photon intensity variation was proportional to the pinhole offset, with the pinhole offsets were 0, 1.5, and 3.5 μ m. The data in the Figure 10 were measured within one hour. It displayed not only the dI_0/I_0 but also the intensity variation of peak-to-peak was proportional to the pinhole offset.

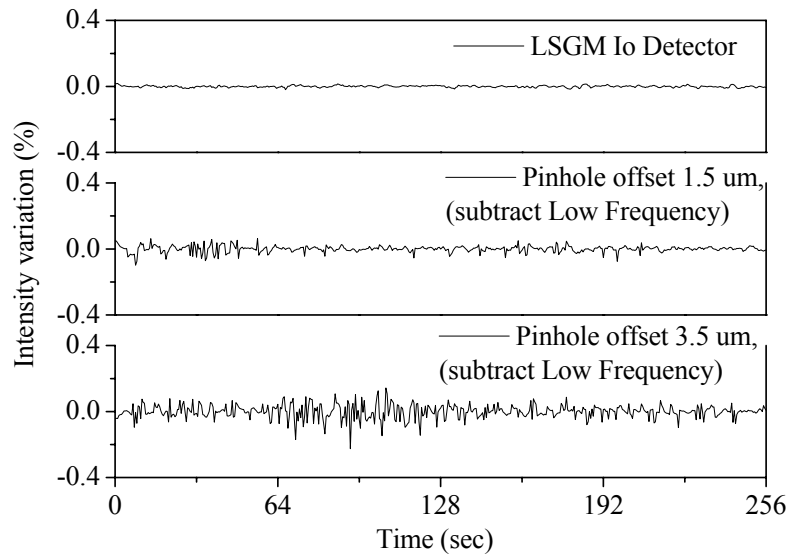


Fig. 9: The intensity variation of high frequency with the offset effect of pinhole.

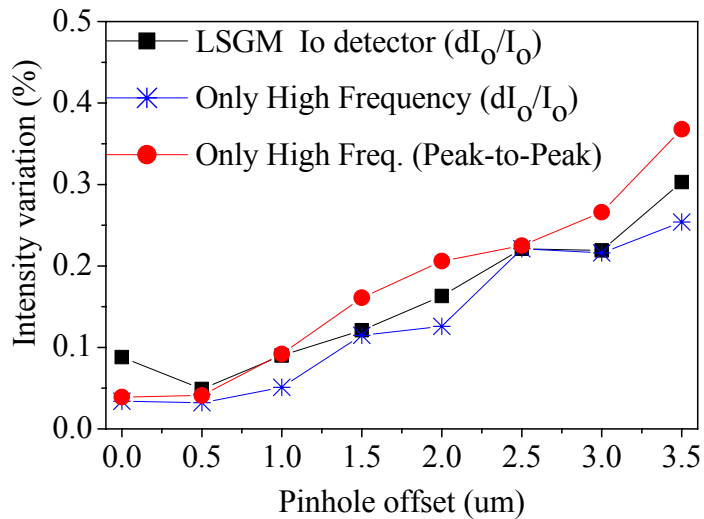


Fig. 10: The intensity variations are proportional to the pinhole offset.

Figure 11 was the performance of this precision I_0 monitor system. The resolution and reliability of this precision I_0 monitor system to indicate the photon beam intensity fluctuation $< 0.1\%$ were proved.

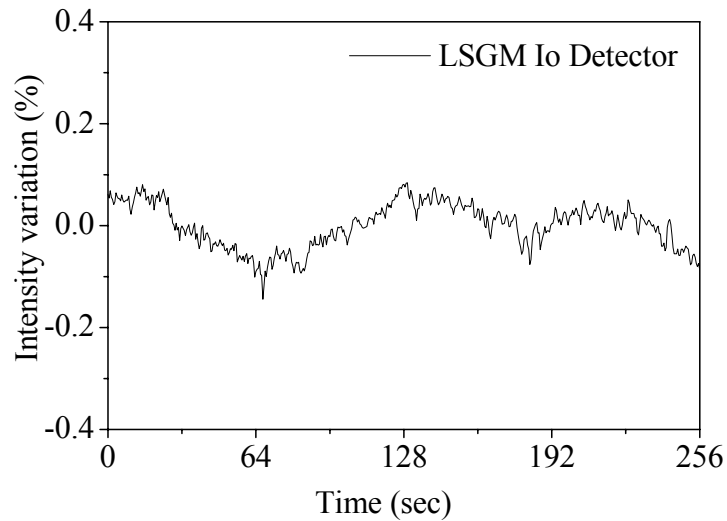


Fig. 11: The performance of this precision I₀ monitor system.

4. Summary

In our study, the mechanical and thermal fluctuations were well controlled by a cooling water system with a temperature fluctuation of $< \pm 0.01$ °C, a AHU with a temperature fluctuation of $< \pm 0.1$ °C, and an independent manipulator. The $0.1\mu\text{m}$ resolution of piezo-actuated flexible stage enhanced the reliability of the precision I₀ monitor system. This precision I₀ monitor was able to indicate the photon beam intensity fluctuation of $< 0.1\%$. After the new intranet program is ready, the data of dI_0/I_0 taken by this precision I₀ monitor system will be archived and be displayed on the TV monitor.

5. Acknowledgments

The authors would like to thank their colleagues, particular the Utility Group for the AHU setting up and the Beam Line Division for valuable information, of the SRRC.

6. References

- [1] T. H. Lee, G. H. Luo, and R. Sah, "Beam Parameters and Automatic Stability Measurement system Using a Pinhole Detector," Proc. of the 1998 Europe Particle Accelerator Conference, Stockholm, Sweden (1998) 605-607.
- [2] G. H. Luo, T. H. Lee, C. K. Kuan, D. J. Wang, "Beam Parameters Measurement by a Pinhole Detector," EPAC'2002, Paris, France (2002) 1930-1932.
- [3] J. R. Chen, D. J. Wang, Z. D. Tsai, C. K. Kuan, S. C. Ho, J. C. Chang, "Mechanical Stability Studies at the Taiwan Light Source," this workshop.
- [4] D. J. Wang, T. C. Tseng, S. Y. Perng, C. K. Kuan, J.R. Chen, "A Compact Mirror Manipulator in the SRRC Beamline," Journal of Synchrotron Radiation (1998), Himeji Japan, (1998) 801-803.